

Visualization Analysis of the Results of Continuum-Atomistic Modeling of a Coulomb Explosion in Metals Under the Influence of Ultrashort (fs, ps) Laser Action

V.I. Mazhukin¹, A.V. Shapranov², M.M. Demin³, O.N. Koroleva⁴, A.V. Mazhukin⁵

Keldysh Institute of Applied Mathematics RAS

- ¹ ORCID: 0000-0001-5590-3731, vim@modhef.ru
² ORCID: 0000-0001-8851-2286, ashapranov@modhef.ru
³ ORCID: 0000-0001-6662-7699, mdemin@mail.ru
⁴ ORCID: 0000-0001-5292-1336, koroleva.on@mail.ru
⁵ ORCID: 0000-0001-7538-6460, specimen@mail.ru

Abstract

A continuum-atomistic model that describes nonequilibrium thermal, hydrodynamic, and electronic processes in metals that occur under the action of ultrashort (fs, ps) laser radiation has been developed. A detailed study of two mechanisms of ultrashort laser ablation of Cu was carried out: fast - Coulomb, determined by Coulomb forces, and slow - thermal, realized in the unloading wave after the end of the laser pulse. Modeling showed that the excess nonequilibrium pressure of collectivized electrons plays a leading role in the formation of a strong electric field at the metal-vacuum interface. This effect can be taken as the basis for the Coulomb explosion in metals. The main feature of the work is the widespread use of modern visualization tools for processing and presenting simulation results.

Keywords: ultrashort laser ablation, Coulomb explosion in metal, continuum-atomistic model, dynamic imaging, electric double layer.

1. Introduction

Ultrashort laser ablation is one of the most promising areas for a wide range of new laser applications in materials science [1], nanotechnology [2, 3], biomedicine [4–6], etc. A detailed study of the mechanisms of ultrashort laser ablation of metals [7, 8] and semiconductors [9, 10] is of great importance for all applications. Due to the large variety of processes involved, which are characterized by a strong spatio-temporal multiscale, such studies present a complex problem. Over the past years, despite the difficulties, not only practical [11, 12] but also fundamental interest [13, 14] still remains in the study of processes initiated by ultrashort laser action.

In experimental studies [15–18], it was found that at least two different mechanisms contribute to the ablation of semiconductors (Si) and metals (Fe, Au, Cu). One mechanism is associated with the release of high-speed particles with an energy of about 5–7 eV. Another mechanism results in the ejection of slow thermal particles with lower energy. Using time-of-flight (TOF) mass spectrometry, bimodal velocity and energy distributions of nanoparticles during femto- and picosecond laser ablation of metals and semiconductors were experimentally measured in these works. It follows from the experiments that the determining factor for the processes under consideration is the time scale on which the laser pulse energy is released in the substance. The observed spectra with a two-peak distribution of particles consisted of two components - a high- and a low-energy component. Obtaining distinct bimodal structures with two different maxima in the velocity and energy distribution of nanoparticles ejected from irradiated metal surfaces indicates that at least two different mechanisms contribute to ultrashort laser ablation. Along with traditional thermal and

hydrodynamic processes, a distinctive feature of ultrashort laser action on metals is the presence of ultrafast electronic processes.

The predominance of thermal and hydrodynamic processes forms the basis of the mechanism of thermal ablation, during which the main removal of matter occurs. This mechanism belongs to the slow ones, since the release and transformation of the laser pulse energy in it occurs on a picosecond time scale.

The mechanism of fast nonthermal ablation is based on fast electronic processes associated with electric fields. Nonthermal ablation occurs near the main ablation threshold and tends to remove hot electrons and accelerated ions from the thin surface layer. Fast electronic processes can lead to the Coulomb explosion (CE), the concepts of the physical mechanisms of which for metals [19, 20] and semiconductors [15, 21, 22] have not been finally formulated and are the subject of considerable scientific interest [23–25].

In the field of determining the dynamic characteristics of laser-induced nonequilibrium processes, the experimental approach, which is traditional, has limitations. Because of this, it is important to use a theoretical approach, the main tool of which is mathematical modeling. At present, two classes of models are most common: continuum, describing phenomena at the macrolevel [26–30] and atomistic, giving an idea of the phenomenon at the microlevel [31–38]. Recently, hybrid continuum-atomistic models have been developed [39, 40], which combine the advantages of continuum models, which make it possible to model electronic excitation under the action of ultrashort laser radiation, and atomistic models, which allow tracking the motion of each molecule or atom, modeling detailed ablation and phase transitions after target irradiation with ultrashort laser radiation impulses. A feature of the action of ultrashort super-powerful laser radiation on metals is the high rate and volumetric nature of energy release in the electronic component, leading to a strong deviation from the state of local thermodynamic equilibrium. The complexity of the mathematical description of the processes induced by laser radiation underlying laser ablation is due to the occurrence of these processes under conditions of strong nonequilibrium, which must be adequately taken into account in theoretical models.

In [26], based on the developed continuum hydrodynamic model, which combines the description of nonequilibrium thermal, hydrodynamic, and electronic processes, a detailed study of the mechanisms of fs-laser ablation of an Al film was performed. The behavior of the electrostatic field was described in terms of an electric double layer (EDL) [27]. The main feature of statement of EDL in the hydrodynamic approximation was the presence of a direct relationship between the electron pressure gradient $\partial P_{e^{ne}}/\partial x$ and the electric field strength E_x , in contrast to drift-diffusion models [23, 24], which makes it possible to study various ablation mechanisms within the framework of a single mathematical model - fast non-thermal, determined by Coulomb forces, and slow, realized in a hydrodynamic unloading wave. Modeling showed that the excess nonequilibrium pressure of collectivized electrons plays a leading role in the formation of a strong electric field at the metal-vacuum interface. This effect can be taken as the basis for the Coulomb explosion in metals.

Validation of the obtained results showed a good qualitative agreement with the experimental data [17, 18]. Further detailing of studies in order to obtain more complete information, including the quantitative component of the occurring phenomena, is associated with the development and application of mathematical models of the microscopic level, called atomistic ones. Typically, an atomistic model consists of $2N$ classical equations of motion, where N is the number particles (atoms, ions) included in the sample under study and is of the order of $(1 - 10) \times 10^6$. The numerical solution of such systems of equations is associated with a large amount of calculations and the complexity of processing and presenting the obtained results.

Considering this circumstance, a continuum-atomistic model was developed to describe the mechanisms of ablation, Coulomb explosion, and spallation of a metal target.

This article presents the results of mathematical modeling of the occurrence of a Coulomb explosion in metals under the influence of fs-ps-laser pulses on the example of copper (Cu), obtained using a new continuum-atomistic model.

A large role in the presentation of the results belongs to visualization. High-quality visualization of the results can enhance the value of the obtained information and begins to play not just the role of displaying (building) images, but is being transformed into a full-fledged component of scientific research. Since the results of mathematical modeling, as a rule, are represented by a large amount of information, their further use for intellectual analysis, demonstration, and training is associated with the need for space-time display of highly unstable regimes of phase transformations, Coulomb explosion, stratification of matter, etc. Recently, the visualization of scientific results has received rapid development [41]. Not a single scientific report, both experimental and theoretical, is published without visualizing the results obtained, mainly using static illustrations. Although dynamic visualization [42, 43] has many more possibilities, which allows illustrating the development of a phenomenon in dynamics, thereby raising the presentation and analysis of scientific results to a qualitatively higher level. Dynamic visualization in scientific publications remains quite rare, since its key difference from static one is the use of animation, as a result of which traditional paper media - books, magazines - no longer correspond to such a representation of information. To use dynamic visualization in the presentation of scientific results in the article, modern multimedia equipment is required, at least what is offered by the most common Internet browsers today. And for the publication of such articles, specialized online publications are needed [44,45].

To present the simulation results obtained in this article, dynamic visualization is used, which makes it possible to show the spatiotemporal evolution of the ablation of a copper target under the influence of ultrashort (fs, ps) laser radiation.

2. Mathematical statement of the problem

The formulation of the problem of laser action on a metal is as follows: a laser radiation flux (Fig. 1) of a Gaussian shape (Fig. 2) is incident on the surface of a metal target (Cu) placed in vacuum along the time coordinate t , wavelength λ , maximum intensity G_0 and duration τ . Part of the radiation is reflected by the surface ($0 < R < 1$, R is the reflection coefficient). The rest of the radiation $A = (1-R)$ is absorbed by the electronic component of the metal. The features of the problem under consideration are determined both by the regime of laser action and by the properties of the irradiated material (metal).

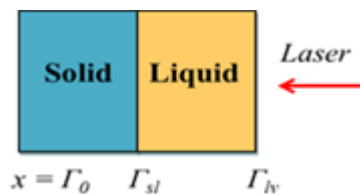


Fig. 1. Scheme of laser action on the target

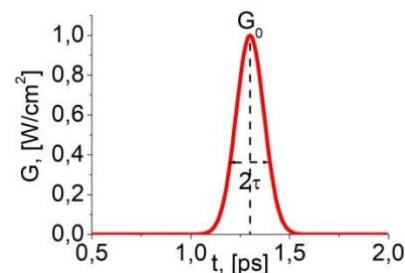


Fig.2. Time profile of the laser pulse
 $G = G_0 \exp(-(t-t_0/\tau)^2)$

The duration of the action of ultrashort pulses turns out to be shorter than the relaxation times of all the main processes, and the absorbed energy of the laser pulse is released in the electronic component, leaving the lattice cold for the time required to transfer energy from heated electrons to the lattice. For this reason, all processes induced by laser radiation: electronic, thermal, hydrodynamic, including phase transformations underlying laser ablation, proceed under conditions of strong nonequilibrium, which must be adequately

taken into account in the mathematical model. One of these effects is the action of the pressure of collectivized electrons in a metal under conditions where the temperatures of the electronic and ionic subsystems differ by tens of thousands of degrees. Accounting for the pressure effect of the electronic component leads to the need to formulate and solve the problem of the electric double layer (EDL), which was considered in detail earlier in [27].

3. Modeling of EDL

According to the quantum mechanical theory of Sommerfeld [46, 47], the electron subsystem is a degenerate Fermi gas of free collectivized electrons. The ionic subsystem consists of heavy positively charged ions, which are considered immobile. In the initial state, it is assumed that the metal is in a state of thermodynamic equilibrium and quasi-neutrality. Collectivized electrons in the thickness of the metal, up to quasi-neutrality, have a constant density ρ_e and freely move through the lattice formed by bound ions. The ions also have a constant density ρ_i up to the boundary with vacuum $x=L$, where the ion density abruptly decreases to zero. Atoms and ions at the vacuum-metal interface (surface) exhibit different properties than atoms and ions in the volume of a phase or material, since they are in a different environment. This is determined primarily by the fact that the surface of a solid metal is always charged, due to the fact that it is formed by the ions that make up the solid.

Under the influence of the pressure of the electronic component P_e , collectivized electrons are squeezed out beyond the metal surface towards vacuum, which leads to the violation of quasi-neutrality and the appearance of an electric field. As a result, the presence of a surface charge leads to the formation of a thin double electric layer formed by two spatially separated layers of electric charges of different signs. The resulting electric field, which prevents the escape of electrons to infinity, contributes to the establishment of electrostatic equilibrium, in which the positive charge of the metal surface is compensated by the negative charge of the electron cloud from the vacuum side.

External action in the form of ultrashort superpower laser pulses on collectivized electrons can lead to a nonlinear response of the electronic component. This effect can be used as the basis for the mechanism of ultrafast (several hundreds of femtoseconds) low-density laser ablation, which was experimentally observed in the studies [15–18]. Under the appropriate conditions, the same effect can lead to a Coulomb explosion.

To represent the electronic processes in the EDL, we used the hydrodynamic description developed in [27] for the continuum model [26]. In this paper, the description of the EDL is adapted for a new hybrid model, which made it possible to obtain a relationship between the nonequilibrium electron pressure gradient and the electric field strength and to explicitly calculate the specific volumetric electric field strength required for the occurrence of a Coulomb explosion.

The main difference between the proposed mathematical formulation of the EDL problem and the widely used drift-diffusion formulations [23, 24] is the presence of a direct relationship between the electron pressure gradient and the electric field. This dependence follows from the hydrodynamic (macroscopic) description of the processes in the EDL. In the quasi-stationary approximation, the mathematical formulation of the EDL is reduced to two problems connected by a common boundary and conventionally called internal and external.

Inside the condensed phase:

$$\begin{cases} \partial P_e(n_e, T_e) / \partial x = -en_e E_x \\ \varepsilon_0 \partial E_x / \partial x = e(zn_0 - n_e) \end{cases} \quad (1)$$

In the outer domain:

$$\begin{cases} \partial P_e(n_e, T_e) / \partial x = -en_e E_x \\ \varepsilon_0 \partial E_x / \partial x = -en_e \end{cases} \quad (2)$$

Boundary conditions:

$$n_e(-\infty)=zn_o, E_x(-\infty)=0 \quad (3)$$

The condition of continuity is satisfied on the metal surface:

$$n_e(\Gamma_{lv}-) = n_e(\Gamma_{lv}+), \quad E_x(\Gamma_{lv}-) = E_x(\Gamma_{lv}+) \quad (4)$$

where accordingly: e , ε_o , E_x are the electron charge, dielectric constant and electric field strength; n_o , z are the concentration of ions in the condensed phase and their degree of ionization; $P_e(n_e, T_e)$ is the total pressure in the electron gas.

4. Combined nonequilibrium continuum-atomistic model

The problem of modeling ultrashort laser action on a metal is described in a single-velocity two-temperature approximation by a combined continuum-atomistic model. For the electron subsystem and the electric double layer (EDL), in contrast to the formulations of other authors [23, 24], the continuum approximation of the hydrodynamic level is used. The molecular dynamics representation is used to describe the motion of heavy particles (ions).

In the atomistic formulation, the computational domain (Fig. 3) in the form of a parallelepiped extended along the X axis is completely filled with particles along the Y, Z -axes, and partially along the X -axis, interacting with each other through the EAM potential developed for copper in [48]. The particles form a single crystal with the corresponding crystal lattice (fcc, bcc). Their average kinetic energy corresponds to an initial temperature of 300 K. Periodic boundary conditions are imposed in the Y and Z directions, thereby reducing 3-D molecular dynamics to a 1-D problem in X .

A laser pulse with intensity G acts from the right to the left along the X axis.

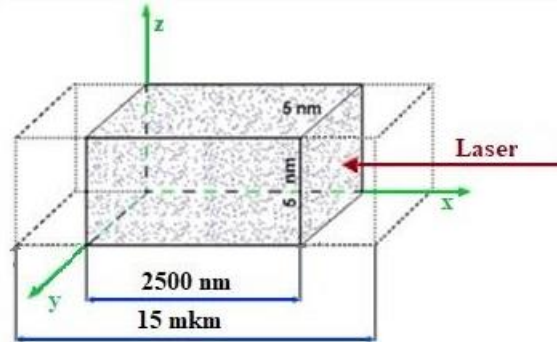


Fig.3. Scheme of the computational experiment at the initial moment of time.

The key element of the method is the choice of the potential (or force) of particle interaction. To date, satisfactory potentials have been developed for a number of metals. However, in the overwhelming majority of cases, they represent an equilibrium situation, just like the equations of state in the continuum approach. Therefore, for the correct formulation of the molecular dynamics problem in the one-velocity two-temperature approximation, the force from the electron subsystem is added to the equations of motion in the form of a gradient of the “non-equilibrium” part of the electron pressure, similarly to the model of a continuous medium

$$\frac{\partial(\varepsilon_e^{ne})}{\partial t} + \frac{\partial(\varepsilon_e^{ne}u)}{\partial x} = - \left(P_e^{ne} \frac{\partial u}{\partial x} + \frac{\partial W_e}{\partial x} + g(T_e)(T_e - T_a) + \frac{\partial G}{\partial x} \right) \quad (5)$$

$$\begin{cases} m_a \frac{d\vec{v}_j}{dt} = \vec{F}_j^{emb} + \vec{J}_j + \left[-\frac{1}{n_a} \frac{\partial P_e^{ne}}{\partial x} \right]_j \vec{e}_x + f_j^{ne} \vec{e}_x \\ \frac{d\vec{r}_j}{dt} = \vec{v}_j, \quad j = 1 \dots N \end{cases} \quad (6)$$

Continual component, equation (5). Designations: $u = \langle v_x \rangle$ is the x -component of the average velocity of the heavy particles, $W_e = -\lambda_e(T_e, T_i) \cdot \partial T_i / \partial x$ is the electron energy flux, $\lambda_e(T_e, T_i)$ is the heat conductivity of electrons; $\partial G / \partial x + \alpha G = 0$ is the equation of laser flux transfer (Beer-Lambert law).

The total energy and pressure of the electron subsystem are divided into “equilibrium” and “nonequilibrium” parts [27]:

$$\begin{aligned} \varepsilon_e &= \varepsilon_e(\rho_e, T_e) = \varepsilon_e^{eq}(T_i) + \varepsilon_e^{ne}(T_i, T_e) \\ P_e &= P_e(\rho_e, T_e) = P_e^{eq}(T_i) + P_e^{ne}(T_i, T_e) \end{aligned} \quad (7)$$

The “equilibrium” (superscript *eq*) parts are considered to be partially included in the thermal and caloric equilibrium equations of state of the metal. “Non-equilibrium” (superscript *ne*) parts are included into the equation (5).

Atomistic component, ODE system (6), describing the motion of heavy particles. Designations: \vec{r}_j, \vec{v}_j are the radius-vector and velocity of the j -th atom, m_a, n_a are the mass and concentration of atoms, \vec{F}_j^{emb} is the force acting on the j -th atom, which is determined by EAM potential, \vec{e}_x is the X -axis unit vector; $\vec{J}_j = m_a(\vec{v}_j - \langle \vec{v} \rangle) g(T_e)(T_e - T_i) / 3k_B T_i n_a$ is the force that ensures the exchange of thermal energy between the electronic and ionic subsystems, T_e, T_i – are the electron and ion temperature; $\langle \vec{v} \rangle$ is the average (hydrodynamic) atom velocity; $g(T_e)(T_e - T_i)$ is the electron-ion coupling term; $b_{xj} = [-1/n_a \cdot \partial P_e^{ne} / \partial x]_j$ – is the electron ion driving force (*blast force*); $\partial P_e^{ne} / \partial x$ – is the gradient of non-equilibrium part of the electron pressure; f_j^{ne} is the force acting on an atom from the excess field of the EDL near the surface of the metal.

The models presented in [49–52], which solve the two-temperature problem by the molecular dynamics method, neglect the work of the electron pressure in the electron energy equation, i.e. term $P_e \cdot \partial u / \partial x$, assuming that its contribution to the total energy balance is insignificant compared to the energy of the laser pulse. The authors carried out a number of calculations that showed that for typical femtosecond regimes of laser action with pulse energies of $\sim 10^{-1} \div 10^0$ J/cm², the energy imbalance introduced without taking into account the work of the electron pressure in the time interval, where the temperature disequilibrium of the subsystems is still large (the picosecond range) is about 12-18%. For this reason, the work of compression forces must be taken into account.

5. Computational algorithm

I step. The hydrodynamic velocity u characterizing the process of electron energy transfer in equation (5) is obtained by averaging the ion velocities in each computational cell. Therefore, the velocity value turns out to be a strongly fluctuating quantity, which complicates the direct numerical solution of the continuum equation (5). Its numerical solution was carried out by the method of total approximation. Each time step consisted of two stages:

At stage – 1: the finite-difference method (explicit-implicit Crank-Nicolson difference scheme on the Euler spatial grid) solves the equation

$$\frac{\partial \varepsilon_e^{ne}}{\partial t} = \frac{\partial}{\partial x} \left(\lambda_e(T_e, T_i) \frac{\partial T_e}{\partial x} \right) - P_e^{ne} \frac{\partial u}{\partial x} - g(T_e)(T_e - T_i) - \frac{\partial G}{\partial x} \quad (8)$$

The positions of atoms and, accordingly, electrons are considered to be frozen.

At stage - 2: the equation of convective transfer is solved, i.e. the continuity equation:

$$\frac{\partial \varepsilon_e^{ne}}{\partial t} + \frac{\partial (\varepsilon_e^{ne} u)}{\partial x} = 0 \quad (9)$$

The solution of (9) is carried out using the molecular dynamics method. To do this, the values of the electronic energy obtained at the first stage in each computational cell are distributed equally among all atoms located in this cell. Then, a molecular dynamic time step is performed, as a result of which heavy particles are displaced in space. Thus, along with the displacement of heavy particles, the electron energy was transferred across the boundaries of the Euler cells. Finally, after summing the electronic energies of the new composition of atoms in each cell (and dividing by the volume of the cell), we obtain the values corrected by transfer of ε_e^{ne} . This completes the two-stage time step for the single-velocity model.

II step. Determination of the spatial dependence of the force f^{ne} acting on an atom from the side of the excess field of EDL near the metal surface. The input data for this problem are n_o, z, T_e . As a result of its solution, the spatial distributions of the electric field E_x and the electron density n_e are obtained at the output.

To determine the force f^{ne} , the problem (1)-(4) is solved twice at each time step of the problem (5)-(6): the first time for the temperature of the electron gas near the surface $T = T_e$, while $E_x(T_e)$ is determined; the second time for a temperature equal to the temperature of the ions near the surface $T = T_i$, in order to determine the value of the electric field $E_x(T_i)$ under the conditions of thermal equilibrium.

Then the specific force included in equation (5) is determined by the excess electric field (in relation to the equilibrium one) and is calculated as follows:

$$f^{ne}(T_e, T_i) = z \frac{e}{m_a} [E_x(T_e) - E_x(T_i)] \quad (10)$$

Here, as above, e is the electron charge, m_a is the ion (atom) mass.

In this case, in the problem (5)-(6) one should use the boundary condition for the electronic component

$$\left. \frac{\partial P_e^{ne}}{\partial x} \right|_{x=\Gamma_{lv}} = 0 \quad (11)$$

since the transfer of momentum from electrons to heavy particles in the near-boundary region has already been taken into account by means of the volume force f^{ne} .

6. Modeling of Coulomb explosion and spallation of the metal target

The results of the modeling the ultrashort laser action on a copper target using the combined continuum-atomistic model in the single-velocity two-temperature approximation (5)-(6) with and without electron pressure (1)-(4) are presented in video 4-7 for the laser action regime of a Gaussian pulse with a duration $\tau = 0.1$ ps and an energy density $J = 1$ J/cm² onto an fcc copper crystal along the (100) direction. The maximum pulse was reached at time $t = 1.3$ ps. In calculations for the atomistic component, the EAM interaction potential for copper was used [48].

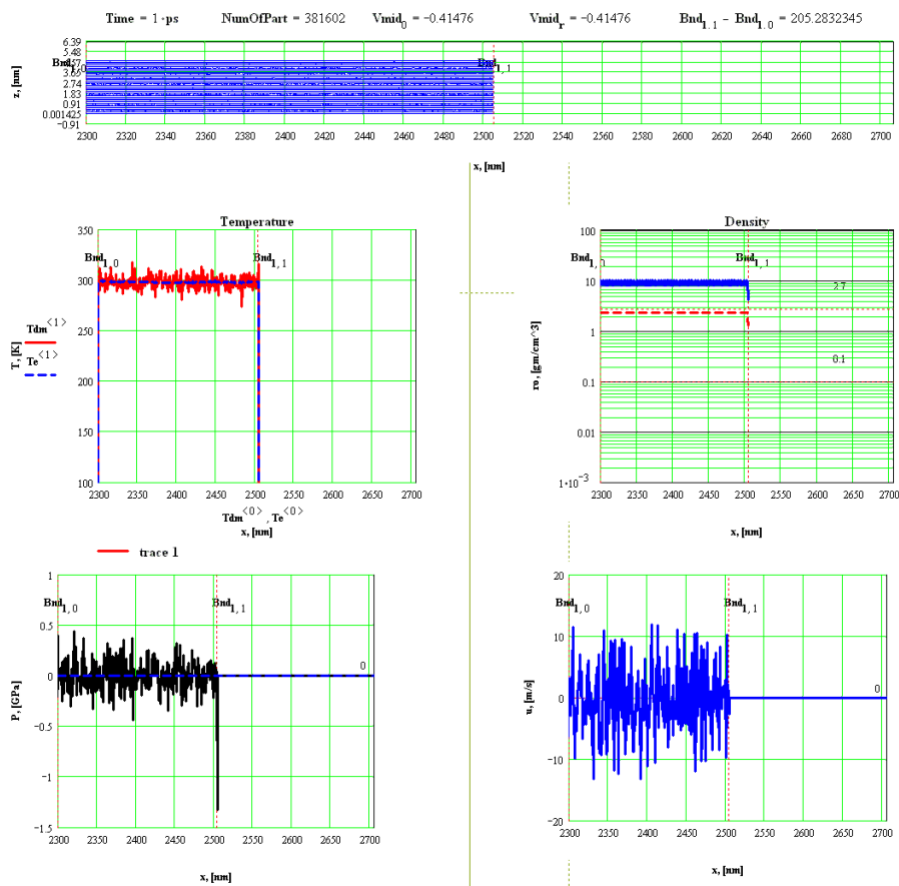
The dynamics of the ablation process is visualized in the presented videos after the time $t = 1$ ps, i.e., the development of the ablation process is shown after the end of the laser pulse and before the end of the process $t > \tau$. For visualization, a MDM screenshot is used, synchronized with the following characteristics of the ablation process: temperatures of electrons T_e and ions T_i ; ion density ρ and order parameter; electronic P_e and ionic P_i pressure; hydrodynamic velocity u of particles and clusters.

The videos demonstrate the ablation process based on the simulation results with electronic pressure (video 4,5) and without it (video 6).

Electron pressure modeling demonstrates a bimodal distribution of particles, showing two ablation mechanisms: fast non-thermal (Coulomb explosion) and slow (thermal-hydrodynamic), which were experimentally observed in [15-18] (video 4).

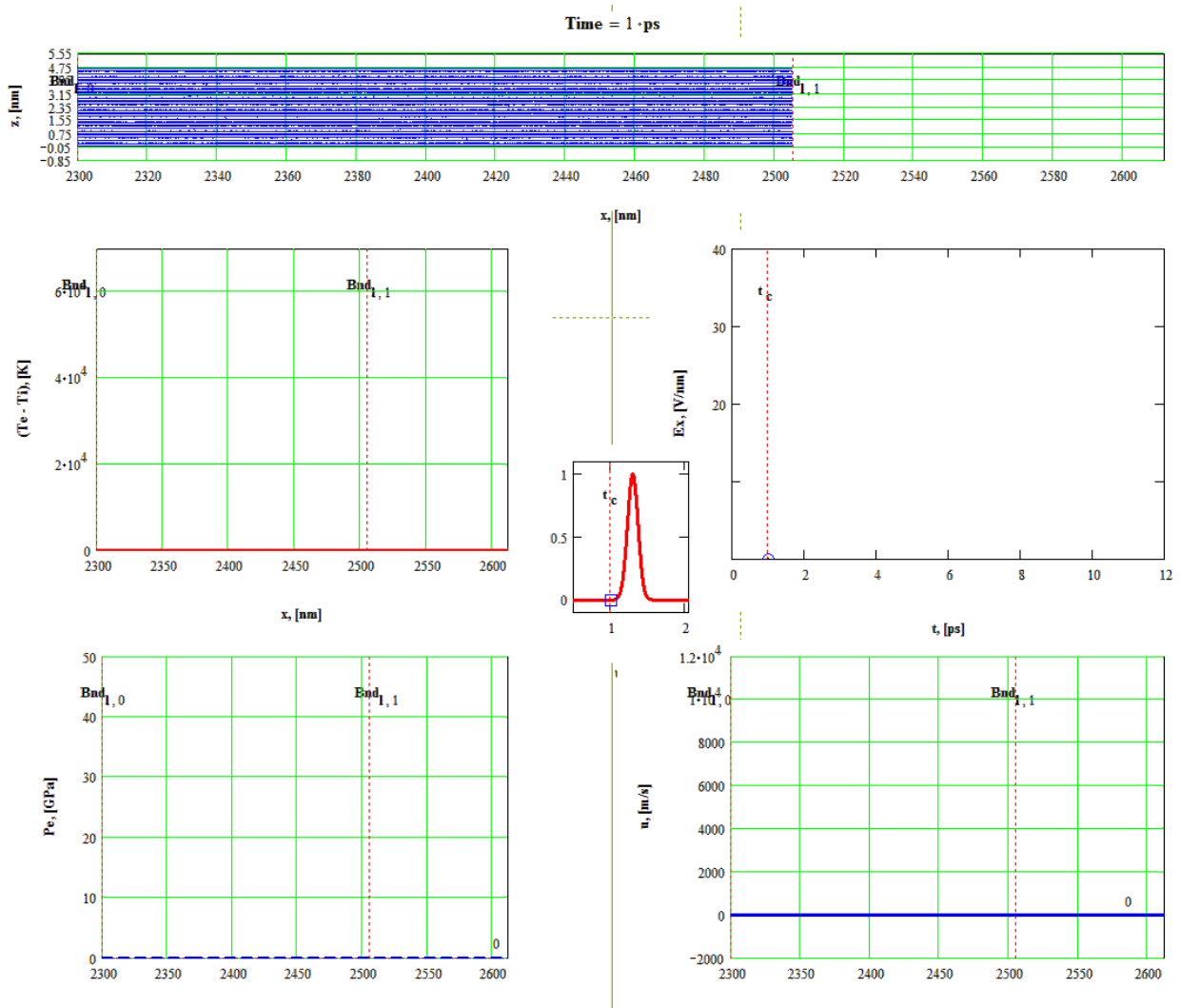
Ultrafast electronic processes leading to a Coulomb explosion according to the simulation results are presented in video 5. In the video presented, the process of ultrafast low-density laser ablation proceeds very quickly, during the time $t = 11$ ps, so the video is built with a small time step $\Delta t = 0.02-0.04$ ps, which makes it possible to study the dynamics of ultrafast electronic processes and the Coulomb explosion.

The picture of the formation of the Coulomb explosion unfolds rapidly, already after $t \approx 0.42$ ps after the end of the pulse, the maximum nonequilibrium of the electron and ion temperatures near the target surface $\Delta T_{max} = T_e - T_i = 6.5 \times 10^4$ K is reached. At that, the “nonequilibrium” part of electron pressure near the target surface also reaches its maximum value $P_e = 47$ GPa and many times exceeds the ion pressure P_i . The maximum value is reached by the electric field $E_x(T_e) = 32$ V/nm. A large electron pressure gradient near the surface in the early expansion phase, already after $t \approx 1$ ps after reaching the maximum values of the characteristics of the explosive ablation process ($t = 2.4$ ps), leads to the detachment of a thin subnanometer surface layer of matter in the form of individual ions and their clusters, which fly at a speed $u = 9000$ m/s. Thus, a Coulomb explosion is observed on the target surface, caused by a large electron pressure gradient in the near-surface layer of the target, the increase of which is provoked by super-powerful ultrashort laser radiation. Subsequently, the expansion velocity increases above 10000 m/s.



Video 4. Simulation results taking into account the Coulomb explosion, 69 ps after the end of the pulse. The characteristics of the ablation process (left to right, top to bottom): electron T_e (blue dashed line) and ion T_i (red solid line) temperature; ion density ρ (blue solid line) and order parameter (red dashed line); “nonequilibrium” pressure of electrons P_e (blue dashed line) and ions P_i (black solid line); hydrodynamic velocity u of particles and clusters (blue solid line).

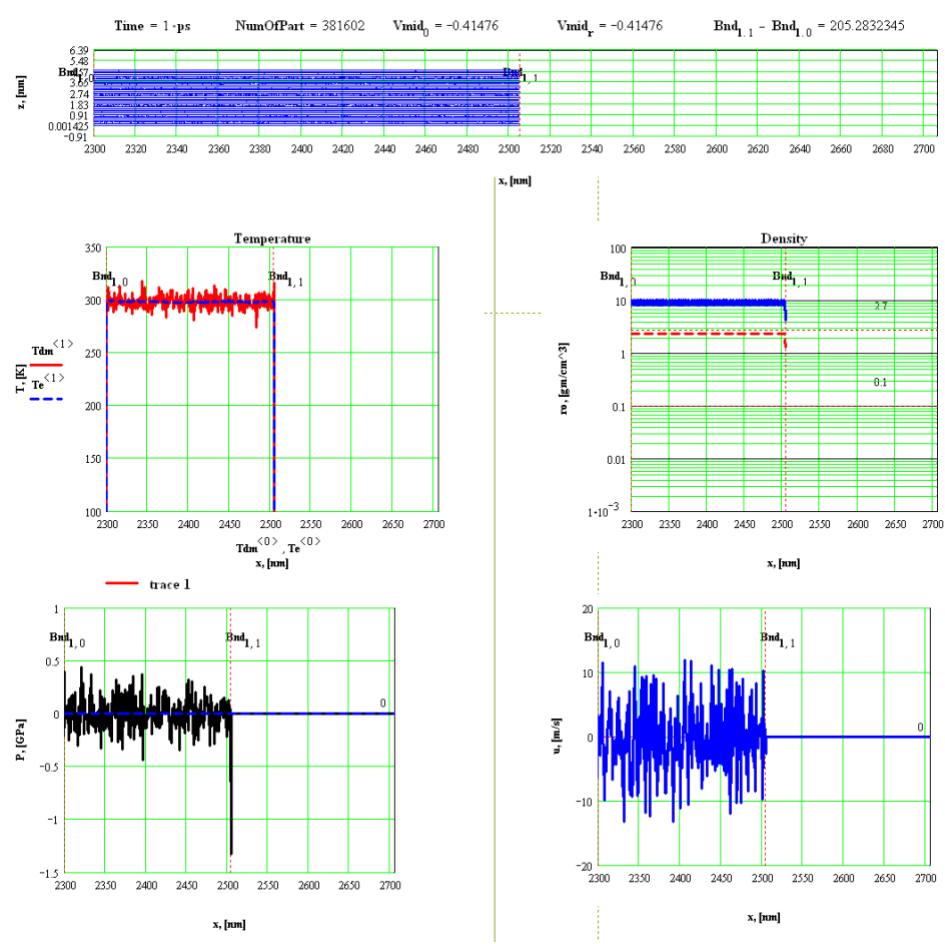
Further (video 4), as the temperature difference of the subsystems decreases, the “non-equilibrium” part of the electron pressure drops rapidly, and a relatively slower process of unloading the ion pressure begins. The electron and ion temperatures equalize, $T_e \approx T_i \approx 5500$ K, at $t = 26$ ps. During this time, a shock wave ($P \approx 28$ GPa) is formed that goes deep into the metal, accompanied by a rarefaction wave (negative pressure reaching $P \approx -5$ GPa). This rarefaction wave causes separation of liquid films with a characteristic thickness of 10–15 nm from the melt, the process beginning at the time $t \approx 38$ ps. The maximum film expansion velocity reaches $u \approx 4000$ m/s.



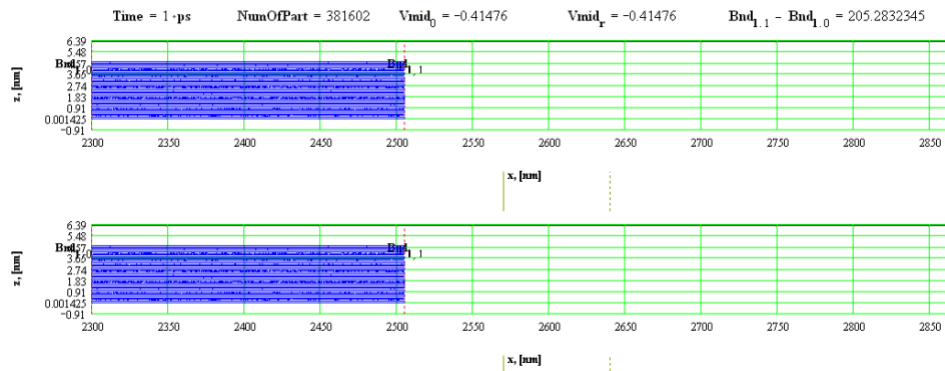
Video 5. Details of the video 4. Dynamics of ultrafast electronic processes and Coulomb explosion, 9.4 ps after the end of the pulse. Characteristics of the process (from left to right, top to bottom): the difference between the electron and ion temperatures at the target surface $\Delta T = T_e - T_i$ (solid red line); electric field strength $E_x(T_e)$ (solid black line); electron pressure P_e (dashed blue line); hydrodynamic velocity u of particles and clusters (solid blue line).

Video 6 shows the results of the modeling the ablation of a copper target without taking into account the influence of the electrical double layer. As we can see, in the initial phase, due to the absence of the action of an additional force caused by a large gradient of electron pressure near the surface, there is no intense expansion of atomic-ion clusters and electrons from the surface of the irradiated target and near it. The process of evaporation from the surface is observed, which is confirmed by a decrease in the density near the surface to $\rho \approx 0.008$ cm⁻³ and by the order parameter. A very small amount of slow fine particles are separated, the speed of which does not exceed $u \leq 4000$ m/s.

Comparison of the simulation results with and without EDL, presented in video 7, shows that the ejection of matter from the target surface is possible only if the EDL is taken into account.



Video 6. Modeling results without taking into account the Coulomb explosion, 86 ps after the start of the pulse. Characteristics of the ablation process (from left to right, top to bottom): electron T_e (dashed blue line) and ion T_i (solid red line) temperatures; ion density ρ (solid blue line) and order parameter (red dashed line); 'non-equilibrium' electronic P_e (dashed blue line) and ionic P_i (solid black line) pressure; hydrodynamic velocity u of particles and clusters (solid blue line).



Video 7. Comparison of modeling results with the Coulomb explosion (upper screenshot) and without the Coulomb explosion (lower screenshot), 70 ps after the end of the pulse.

7. Conclusions

The Coulomb explosion is one of the electronic mechanisms of laser ablation, which has been widely discussed in the last few decades [19-25] and observed in experiments [15-18]. In

this article, to study the possibility of implementing a Coulomb explosion in metals, a new combined continuum-atomistic model was proposed and developed, and the results of mathematical modeling of a Coulomb explosion under the influence of fs-ps laser pulses in a copper target are presented.

A new mathematical description of ultrashort laser action on a metal is carried out in a single-velocity two-temperature approximation by a combined continuum-atomistic model. For the electron subsystem and the electric double layer (EDL), in contrast to the formulations of other authors [23, 24], the continuum approximation of the hydrodynamic level is used. The molecular dynamics representation is used to describe the motion of heavy particles (ions).

The hydrodynamic description developed in [27] was used to represent the electronic processes in the EDL. In [26], this description was used in the continuum model, and in the present work it was adapted for a new hybrid model, which made it possible to obtain a relationship between the nonequilibrium electron pressure gradient and the electric field strength and to explicitly calculate the specific volumetric electric field strength required for the occurrence of a Coulomb explosion.

With the help of a new continuum-atomistic model, an extensive study of various regimes of laser fs, ps action on a Cu target has been carried out. Two ablation mechanisms were obtained, which are observed in the experiments [15-18] - a fast nonthermal one, determined by Coulomb forces, and a slow one, realized in a hydrodynamic unloading wave.

In the study of the modeling results, a significant role is played by their visualization, which gives a visual representation of the evolution of the process of laser ablation of a copper target under the influence of ultrashort (fs, ps) high-power laser pulses. Understanding and interpreting the modeling results is a non-trivial task for any category of researchers, not only because of the large volume of results obtained, but also because of the wide variety of simulated processes, which are characterized by a strong spatio-temporal scale. Animation, one of the methods of dynamic visualization, was used to facilitate the understanding of the results obtained, representing a series of arrays of large numerical values.

The use of animation allowed us:

- to study in detail the dynamics of the bimodal process of laser ablation of a copper target.
- to present in detail both the ultrafast mechanism of laser ablation - the Coulomb explosion (video 5), which proceeds for a very short time of $t = 11$ ps, and the slow thermal mechanism of target spallation (video 4),
- to study the patterns, obtain quantitative characteristics of the processes,
- to visualize the comparison of the simulation results with and without the electrical double layer, presented in videos 4, 6, 7, which showed that the release of the substance from the target surface is possible only with the electrical double layer taken into account.

The use of dynamic visualization to present the results of mathematical modeling helped to reduce the cognitive load associated with their complexity, facilitating understanding, research and analysis [42].

In the scientific problem under consideration, dynamic visualization has become not only a means of presenting simulation results, but also a full-fledged tool for scientific research.

Acknowledgements

The results were obtained using the equipment of Shared Resource Center of KIAM RAS (<http://ckp.kiam.ru>). The work was supported by Russian Science Foundation, grant No. 18-11-00318.

References

1. Nanomaterials: Processing and Characterization with Lasers, S. Ch. Singh, H.B. Zeng, Ch. Guo, W. Cai (Eds.), Weinheim:Wiley-VCH, 2012.

2. Zhang Z., Xu Z., Wang C., Liu S., Yang Z., Zhang Q., Xu W. Molecular dynamics-guided quality improvement in the femtosecond laser percussion drilling of microholes using a two-stage pulse energy process. // *Optics & Laser Technology*, Vol. 139, 2021, 106968. (doi:10.1016/j.optlastec.2021.106968)
3. Chichkov B.N. Laser printing: trends and perspectives. // *Appl. Phys. A*, Vol. 128, 2022, 1015. (doi:10.1007/s00339-022-06158-9)
4. Elahi N., Kamali M., Baghersad M.H. Recent biomedical applications of gold nanoparticles: A review. // *Talanta*, Vol. 184, 2018, 537-556. (doi:10.1016/j.talanta.2018.02.088)
5. Fadeeva E., Schlie-Wolter S., Chichkov B.N., Paasche G., Lenarz T. Structuring of biomaterial surfaces with ultrashort pulsed laser radiation. // *Laser Surface Modification of Biomaterials*, 2016, 145–172. (doi:10.1016/b978-0-08-100883-6.00005-8)
6. Jendrzey S., Gökce B., Epple M., Barcikowski S. How Size Determines the Value of Gold: Economic Aspects of Wet Chemical and Laser-Based Metal Colloid Synthesis. // *ChemPhysChem*, Vol. 18, No. 9, 2017, 1012–1019. (doi:10.1002/cphc.201601139)
7. Gamaly E.G. *Femtosecond Laser-Matter Interaction: Theory, Experiments and Applications*. Boca Raton: CRC Press, 2011. (doi: 10.1201/9789814267809)
8. Mazhukin A.V., Mazhukin V.I., Demin M.M. Modeling of femtosecond laser ablation of Al film by laser pulses. // *Appl. Surf. Sci.*, 2011, No. 257, 5443–5446. (doi:10.1016/j.apsusc.2010.11.154)
9. Ovchinnikov A.V., Chefonov O.V., Agranat M.B., Kudryavtsev A.V., Mishina E.D., Yurkevich A.A. Free-carrier generation dynamics induced by ultrashort intense terahertz pulses in silicon. // *Optics Express*, Vol. 29, No. 16, 2021, 26093-26102. (doi:10.1364/OE.430752)
10. Moser R., Domke M., Winter J., Huber H.P., Marowsky G. Single pulse femtosecond laser ablation of silicon – a comparison between experimental and simulated two-dimensional ablation profiles. // *Adv. Opt. Techn.*, Vol. 7, No. 4, 2018, 1-10. (doi:10.1515/aot-2018-0013)
11. Menéndez-Manjón A., Barcikowski S., Shafeev G.A., Mazhukin V.I., Chichkov B.N. Influence of beam intensity profile on the aerodynamic particle size distributions generated by femtosecond laser ablation. *Laser and Particle Beams*, Vol. 28, No. 1, 2010, 45 - 52. (doi:doi:10.1017/S0263034609990553)
12. Gamaly E.G., Rode A.V. Physics of ultra-short laser interaction with matter: From phonon excitation to ultimate transformations. // *Progress in Quantum Electronics*, Vol. 37, No. 5, 2013, 215–323. (doi: 10.1016/j.pquantelec.2013.05.001)
13. Mazhukin V.I. Kinetics and Dynamics of Phase Transformations in Metals Under Action of Ultra-Short High-Power Laser Pulses. Chapter 8, // *Laser Pulses – Theory, Technology, and Applications*, 2012, I. Peshko (Ed.), InTech, Croatia, 219 -276 (doi:10.5772/50731)
14. Wang B., Wang Y., Song H., Lam Y.C., Shaymaa E.M., Liu S. Threshold effect on the femtosecond laser-induced periodic subwavelength structure: An analytical approach. // *Optics & Laser Technology*, Vol. 158, Part A, 2023, 108804. (doi:10.1016/j.optlastec.2022.108804).
15. Roeterdink W.G., Juurlink L.B.F., Vaughan O.P.H., Dura Diez J., Bonn M., Kleyn A.W. Coulomb explosion in femtosecond laser ablation of Si(111). // *Appl. Phys. Lett.*, Vol. 82, No. 23, 2003, 4190–4192. (doi:10.1063/1.1580647)
16. Cheng H.-P., Gillaspay J.D. Nanoscale modification of silicon surfaces via Coulomb explosion. // *Phys. Rev. B*, Vol. 55, No. 4, 1997, 2628–2636. (doi:10.1103/physrevb.55.2628)
17. Dachraoui Hatem, Husinsky Wolfgang. Fast electronic and thermal processes in femtosecond laser ablation of Au. // *Appl. Physics Lett.*, Vol. 89, 2006, 104102.
18. Dachraoui H., Husinsky W., Betz G. Ultra-short laser ablation of metals and semiconductors: evidence of ultra-fast Coulomb explosion. // *Appl. Phys. A*, Vol. 83, 2006, 333–336. (doi: 10.1007/s00339-006-3499-y)

19. Vella A., Deconihout B., Marrucci L., Santamato E., Femtosecond Field Ion Emission by Surface Optical Rectification. // *Phys. Rev. Lett.*, Vol. 99, No. 4, 2007, 046103-4. (doi:10.1103/physrevlett.99.046103)
20. Shuchang Li, Suyu Li, Fangjian Zhang, Dan Tian, He Li, Dunli Liu, Yuanfei Jiang, Anmin Chen, Mingxing Jin. Possible evidence of Coulomb explosion in the femtosecond laser ablation of metal at low laser fluence. // *App. Surf. Sci.*, Vol. 355, 2015, 681-685. (doi: 10.1016/j.apsusc.2015.07.136)
21. Cheng Hai-Ping, Gillaspay J.D. Nanoscale modification of silicon surfaces via Coulomb explosion. // *Phys. Rev. B*, Vol. 55, No. 4, 1997, 2628 - 2636. (doi:10.1103/PhysRevB.55.2628)
22. Stoian R., Rosenfeld A., Hertel I.V., Bulgakova N.M., Campbell E.E. Comment on "Coulomb explosion in femtosecond laser ablation of Si(111)" [*Appl. Phys. Lett.*, 82, 4190 (2003)]. // *Appl. Phys. Lett.*, Vol. 85, No. 4, 2004, 694-695. (doi:10.1063/1.1771817)
23. Bulgakova N.M., Stoian R., Rosenfeld A., Marine W., Campbell E.E. A general continuum approach to describe fast electronic transport in pulsed laser irradiated materials: the problem of Coulomb explosion. // *High-Power Laser Ablation V*, Proceedings of SPIE, Vol. 5448, 2004, 121-135. (doi:10.1117/12.548823)
24. Tao Sha, Wu Benxin. The effect of emitted electrons during femtosecond laser-metal interactions: A physical explanation for coulomb explosion in metals. // *App. Surf. Sci.*, Vol. 298, 2014, 90-94.
25. Shugaev M.V., Wu C., Armbruster O., Naghilou A., Brouwer N., Ivanov D.S., Zhigilei L.V. Fundamentals of ultrafast laser-material interaction. // *MRS Bulletin*, Vol. 41, No. 12, 2016, 960-968.
26. Mazhukin V.I., Demin M. M., Shapranov A.V., Mazhukin A.V. Role of electron pressure in the problem of femtosecond laser action on metals. // *Appl. Surf. Sci.*, Vol. 530, 2020, 147227. (doi: 10.1016/j.apsusc.2020.147227)
27. Mazhukin V.I., Shapranov A.V., Mazhukin A.V. The structure of the electric double layer at the metal-vacuum interface. // *Math. Montis.*, Vol. 44, 2019, 110-121. (doi: 10.20948/mathmon-2019-44-9)
28. Mazhukin V.I., Shapranov A.V., Mazhukin A.V., Koroleva O.N. Mathematical formulation of a kinetic version of Stefan problem for heterogeneous melting/crystallization of metals. // *Math. Montis.*, Vol. 36, 2016, 58-77.
29. Jia Xiao, Zhao Xin. Numerical study of material decomposition in ultrafast laser interaction with metals. // *App. Surf. Sci.*, Vol. 463, 2019, 781-790.
30. Xiang M., Jiang S., Cui J., Xu Y., Chen J. Coupling of dynamic ductile damage and melting in shock-induced micro-spalling: Modeling and applications. // *Int. J. Plast.*, Vol. 136, 2021, 102849. (doi:10.1016/j.ijplas.2020.102849)
31. Mazhukin V.I., Shapranov A.V., Mazhukin A.V., Breslavsky P.V. Atomistic modeling of the dynamics of the solid/liquid interface of Si melting and crystallization taking into account deeply superheated/supercooled states. // *Math. Montis.*, Vol. 47, 2020, 87-99. (doi: 10.20948/mathmontis-2020-47-8)
32. Mazhukin V. I., Koroleva O. N., Shapranov A. V., Demin M. M., Aleksashkina A. A. Determination of thermal properties of gold in the region of melting-crystallization phase transition: molecular dynamics approach. // *Math. Models Comput. Simul.*, Vol. 14, No. 4, 2022, 662-676. (doi: 10.1134/S2070048222040068)
33. Mazhukin V. I., Koroleva O. N., Demin M. M., Shapranov A. V., Aleksashkina A. A. Atomistic Simulation of the Coexistence of Liquid-Vapor Phase States for Gold and Determination of Critical Parameters. // *Math. Models Comput. Simul.*, Vol. 14, No. 5, 2022, 819-828. (doi: 10.1134/S207004822205009X)
34. Mazhukin V.I., Samokhin A.A., Shapranov A.V., Demin M.M. Modeling of thin film explosive boiling - surface evaporation and electron thermal conductivity effect. // *Mater. Res. Express*, Vol. 2-1, 2015, 016402 (1-9). (doi:10.1088/2053-1591/2/1/016402)

35. Mazhukin V.I., Samokhin A.A., Demin M.M., Shapranov A.V. Explosive boiling of metals upon irradiation by a nanosecond laser pulse. // *Quantum Electronics*, Vol. 44, No. 4, 2014, 283–285.
36. Shih C.Y., Streubel R., Heberle J., Letzel A., Shugaev M.V., Wu C., Zhigilei L.V. Two mechanisms of nanoparticle generation in picosecond laser ablation in liquids: the origin of the bimodal size distribution. // *Nanoscale*, Vol. 10, No. 15, 2018, 6900–6910. (doi:10.1039/c7nr08614h)
37. Pariz I., Goel S., Nguyen D. T., Buckeridge J., Zhou X. A critical review of the developments in molecular dynamics simulations to study femtosecond laser ablation. // *Materials Today: Proceedings*, Vol. 64, No. 3, 2022, 1339-1348. (doi: 10.1016/j.matpr.2022.03.723)
38. Demin M.M., Koroleva O.N., Aleksashkina A.A., Mazhukin V.I. Molecular-dynamic modeling of thermophysical properties of phonon subsystem of copper in wide temperature range. // *Math. Montis.*, Vol. 47, 2020, 137 - 151. (doi: 10.20948/mathmontis-2020-47-12).
39. Li X., Guan Y. Theoretical fundamentals of short pulse laser–metal interaction: A review. // *Nanotechnol. Precis. Eng.*, Vol. 3, 2020, 105-125. (doi:10.1016/j.npe.2020.08.001)
40. Meng Yu., Ji P., Jiang L., Lin G., Guo J. Spatiotemporal insights into the femtosecond laser homogeneous and heterogeneous melting aluminum by atomistic-continuum modeling. // *Appl. Phys. A*, Vol. 128, 2022, 520. (doi: 10.1007/s00339-022-05610-0)
41. Yao J., Qi D., Liang H., He Y., Yao Y., Jia T., Yang Y., Sun Z., Zhang S. Exploring Femtosecond Laser Ablation by Snapshot Ultrafast Imaging and Molecular Dynamics Simulation. // Vol. 2022, 2022, Article ID 9754131, 1-11. (doi: 10.34133/2022/9754131)
42. Aysolmaz Banu, Reijers Hajo A. Animation as a dynamic visualization technique for improving process model comprehension. // *Information & Management*, Vol. 58, No. 5, 2021, 103478. (doi: 10.1016/j.im.2021.103478)
43. Ahmed A., Fu X., Hong S.H., Nguyen Q.H., Xu K. Visual Analysis of History of World Cup: A Dynamic Network with Dynamic Hierarchy and Geographic Clustering. // *Visual Information Communication*. Springer, Boston, MA, 2009. (doi.org/10.1007/978-1-4419-0312-9_2)
44. Mazhukin V.I., Samokhin A.A., Shapranov A.V., Demin M.M., Pivovarov P.A. Modeling and visualization of nanosecond laser vaporization of metals in near critical region. // *Scientific Visualization*, Vol. 8, No 1, 2016, 1-22.
45. Breslavskiy P.V., Koroleva O.N., Mazhukin A.V. The evolution of the plasma formation in the gas medium, modeling with visualization of the grid nodes dynamics and the interaction of shock and thermal waves. // *Scientific Visualization*, Vol.7, No. 5, 2015, 1-11.
46. Bete G. and Sommerfeld A. *Electronic Theory of Metals*, Springer, Berlin, 1933.
47. Ashcroft N.W. and Mermin N.D. *Solid State Physics*. W. B. Saunders Co., 1976.
48. Mishin Y., Mehl M.J., Papaconstantopoulos D.A., Voter A.F., Kress J.D. Structural stability and lattice defects in copper: Ab initio, tight-binding, and embedded-atom calculations // *Phys. Rev. B*, Vol. 63, 2001, 224106.
49. Lin Z., Leveugle E., Bringa E.M., Zhigilei L.V., Molecular Dynamics Simulation of Laser Melting of Nanocrystalline Au. // *The Journal of Physical Chemistry C*, Vol. 114, No. 12, 2009, 5686–5699. (doi:10.1021/jp909328q)
50. Povarnitsyn M. E., Itina T. E., Sentis M., Khishchenko K. V., and Levashov P. R. Material decomposition mechanisms in femtosecond laser interactions with metals. // *Phys. Rev. B*, Vol. 75, 2007, 235414.
51. Mazhukin V.I., Demin M.M., Shapranov A.V. High-speed laser ablation of metal with pico- and subpicosecond pulses. // *Appl. Surf. Sci.*, Vol. 302, 2014, 6–10.
52. Shugaev M.V., Zhigilei L.V. Thermodynamic analysis and atomistic modeling of subsurface cavitation in photomechanical spallation. // *Comput. Mater. Sci.*, Vol. 166, 2019, 311-317. (doi:10.1016/j.commatsci.2019.05.017).